Received: 30 November 2022 | Revised: 7 February 2023 | Accepted: 12 March 2023

DOI: 10.1002/bit.28381

COMMUNICATION

BIOTECHNOLOGY BIOENGINEERING WILEY

Preservation of critical quality attributes of mesenchymal stromal cells in 3D bioprinted structures by using natural hydrogel scaffolds

Lluís Martorell[1] | Alba López-Fernández[1,2] | Andrea García-Lizarribar[3] | Roger Sabata[4] | Patricia Gálvez-Martín[4] | Josep Samitier[3,5,6] | Joaquim Vives[1,2,7]

[1]Banc de Sang i Teixits, Edifici Dr. Frederic Duran i Jordà, Barcelona, Spain

[2]Musculoskeletal Tissue Engineering Group, Vall d'Hebron Research Institute (VHIR), Universitat Autònoma de Barcelona, Barcelona, Spain

[3]Institute for Bioengineering of Catalonia (IBEC), Barcelona Institute of Science and Technology (BIST), Barcelona, Spain

[4]R&D Human Health, Bioibérica S. A. U., Barcelona, Spain

[5]Department of Electronics and Biomedical engineering, University of Barcelona, Barcelona, Spain

[6]Biomedical Research Networking Center in Bioengineering, Biomaterials, and Nanomedicine (CIBER-BBN), Madrid, Spain

[7]Departament de Medicina, Universitat Autònoma de Barcelona, Barcelona, Spain

Correspondence
Joaquim Vives
Email: jvives@bst.cat

Josep Samitier
Email: jsamitier@ibecbarcelona.eu

Funding information
Catalonia Trade & Investment; Generalitat de Catalunya; Instituto de Salud Carlos III

Abstract

Three dimensional (3D) bioprinting is an emerging technology that enables complex spatial modeling of cell-based tissue engineering products, whose therapeutic potential in regenerative medicine is enormous. However, its success largely depends on the definition of a bioprintable zone, which is specific for each combination of cell-loaded hydrogels (or bioinks) and scaffolds, matching the mechanical and biological characteristics of the target tissue to be repaired. Therefore proper adjustment of the bioink formulation requires a compromise between: (i) the maintenance of cellular critical quality attributes (CQA) within a defined range of specifications to cell component, and (ii) the mechanical characteristics of the printed tissue to biofabricate. Herein, we investigated the advantages of using natural hydrogel-based bioinks to preserve the most relevant CQA in bone tissue regeneration applications, particularly focusing on cell viability and osteogenic potential of multipotent mesenchymal stromal cells (MSCs) displaying tripotency in vitro, and a phenotypic profile of 99.9% $CD105^{+}$/$CD45,^{-}$ 10.3% $HLA\text{-}DR,^{+}$ 100.0% $CD90,^{+}$ and 99.2% $CD73^{+}$/$CD31^{-}$ expression. Remarkably, hyaluronic acid, fibrin, and gelatin allowed for optimal recovery of viable cells, while preserving MSC's proliferation capacity and osteogenic potency in vitro. This was achieved by providing a 3D structure with a compression module below 8.8 ± 0.5 kPa, given that higher values resulted in cell loss by mechanical stress. Beyond the biocompatibility of naturally occurring polymers, our results highlight the enhanced protection on CQA exerted by bioinks of natural origin (preferably HA, gelatin, and fibrin) on MSC, bone marrow during the 3D bioprinting process, reducing shear stress and offering structural support for proliferation and osteogenic differentiation.

Lluís Martorell, Alba López-Fernández, and Andrea García-Lizarribar contributed equally to this work.

KEYWORDS
3D bioprinting, critical quality attributes, human mesenchymal stromal cells, osteogenic differentiation, potency, substances of human origin (SoHO)

1 | INTRODUCTION

Three dimensional (3D) bioprinting is an emerging technology that enables the modeling of complex cell-based tissue engineering products (TEP) with clinical potential in regenerative medicine applications (Murphy & Atala, 2014). 3D bioprinting can be implemented in the context of advanced therapy medicinal product (ATMP) development. ATMPs are medicines for human use based on the manipulation of genes, tissues or cells, offering ground-breaking new opportunities for the treatment of disease and injury. However, ATMP manufacture is mostly done in the nonindustrial setting following manual operations with little automation, particularly in TEP production. In this context, 3D bioprinting is a suitable solution to (i) avoid the use of molds to generate unique tissue architectures, and (ii) automate the fabrication process of clinically relevant 3D shaped cell-based structures, by an additive manufacturing approach allowing layer by layer-controlled deposition of biomaterials loaded with cells (bioink) and/or biomaterials to support the structure. The formulation of a bioink involves the mix of living cells with a carrier biomaterial (initially in a liquid state, although viscous) that subsequently solidifies, allowing biofabricate a wide range of shapes. Throughout the bioprinting process, the integrity of living cells can be damaged, decreasing cell viability and altering the biological and structural characteristics of the bioprinted TEP. The most common approaches to bioprint a TEP are: (i) inkjet-based 3D bioprinting, (ii) stereolithographic-based 3D bioprinting (SLA), (iii) laser 3D bioprinting, and (iv) extrusion-based bioprinting (EBB) (Abu Owida, 2022; Jose et al., 2016). EBB is the most convenient and scalable bioprinting technique of TEP. In EBB, the bioink is charged in a printing syringe, which is placed in one of the heads of the bioprinter and the X, Y, and Z dimensional movements of the bioprinter are controlled by a computer-aided design software, shaping the 3D structure of the desired tissue. Then, the bioprinter extrudes the bioink using air or mechanical pressure to draw the designed tissue. EBB provides several advantages over other techniques such as: (i) allowing the use of bioinks with higher viscosity which are bioprinted as filaments through the needle and can maintain this shape after their deposition (post-bioprinting), (ii) offers a greater cell coverage and helps maintaining cell viability of TEP, (iii) greater precision, (iv) faster bioprinting speed, and (v) versatility to bioprint a wider range of biomaterials (Abu Owida, 2022). However, the use of highly bioprintable bioinks is associated to low cell viability recovery. In contrast, low viscous solutions are extruded as drops. These drops don't preserve the filament shape of the needle, since they expand, and collapse with previously bioprinted lines, resulting in poorly defined 3D structures but, in contrast, cell viability is preserved. Thus, it is necessary to guarantee a balance between bioink printability (resolution and mechanical properties) and cellular characteristics (identity and potency), also referred as the "bioprintable zone," which should allow bioprinting a TEP with adequate spatial resolution and with a compromise of cell recovery and maintenance of viability (as well as other critical quality attributes [CQA]) (Cidonio et al., 2019). To date, highly bioprintable materials have been used to simplify the fabrication process (save in time and material). However, commonly used natural biomaterials such as gelatin and alginate at high concentration, for instance, offer high stiffness and this impacts negatively on the proliferation and migration capacity of cells. Therefore, one of the major limitations in 3D bioprinting of TEPs for effective translation into the clinics is the optimization of bioink formulations to mimic the cells physiological conditions (Donnaloja et al., 2020). Thus, in spite of the advantages of 3D bioprinting to fabricate TEP, not a single ATMP utilizing such approach has been authorized for human use yet, mostly due to the challenge of finding suitable bioink formulations to bioprint tissues with adequate biological and structural properties similar to the tissues to be replaced.

Herein we formulated different hydrogels from natural biomaterials (including gelatin, hyaluronic acid [HA], glycerol, fibrin) combined with multipotent mesenchymal stromal cells (MSC) as bioinks for bone tissue regeneration. The qualities of MSC are of great interest in innovative therapies, including bone tissue regeneration upon transplantation in patients suffering trauma, infection, or degenerative conditions provided that MSC: (i) hold the potential to differentiate into mesenchymal lineages (e.g., osteoblasts, chondroblasts, adipocytes); and (ii) are capable to respond to local inflammatory microenvironment (Dimarino et al., 2013; Vives & Mirabel, 2019). In the present research, we investigated the effect of clinical grade MSC-loaded bioinks on major CQA (cell viability, proliferative capacity, osteogenic differentiation potential, and dimensional accuracy) in 3D printed grid-shaped constructs, as model system.

2 | MATERIALS AND METHODS

2.1 | Experimental design

An experimental matrix was defined to test suitable combinations of hydrogels, which were chosen based on prior preclinical and clinical experience in the generation of (non-3D printed) osteogenic MSC-based TEP, as reported elsewhere (García de Frutos et al., 2020; Prat et al., 2018; Vivas et al., 2020; Vives et al., 2021). Particularly: clinical grade fibrin (Tissucol Duo; Baxter) as a result from mixing fibrinogen and 1:100 diluted thrombin at 5 UI/mL final concentration in saline solution (Viaflo Plasmalyte 148; Baxter) supplemented with 2% human serum albumin (HSA; Albutein®; Grifols); clinical grade HA

(Bioiberica) dissolved either at 1% or 5% (w/v) in warm saline solution and sterilized by filtration with a 0.45 µm Millex-HV filter (Merck Millipore) or by autoclaving, respectively; and research grade polymer precursors of gelatin and alginate methacryloyl (GelMA and AlgMA, respectively) (Sigma-Aldrich) were altered to a 40% methacrylation degree. Shortly, the gelatin was dissolved at a concentration of 10% (w/v) in 10 mM phosphate buffered saline (PBS; Sigma-Aldrich) and methacrylic anhydride (Sigma-Aldrich) was added dropwise under constant stirring. After 1 h, 10 mM PBS was added to stop the reaction reaching a 5x dilution. The solution was then dialyzed against Milli Q water in 3.5 kDa SnakeSkin membranes (Thermo Fisher Scientific) for 3 days at 40°C. The methacrylation of sodium alginate was performed by dissolving sodium alginate (1% w/v) (Sigma-Aldrich) in 50 mM 2-(N-morpholino)ethanesulfonic acid (MES; Sigma-Aldrich) buffer at pH 6.5 as well as 20 mM of N-(3-Dimethylaminopropyl)-N'-ethylcarbodiimide hydrochloride (EDC; Sigma-Aldrich) and 10 mM N-hydroxysuccinimide (Sigma-Aldrich) followed, after 10 min, by the addition of 10 mM 2-aminoethylmethacrylate (Sigma-Aldrich). After 24 h at 40°C, acetone (Panreac) was used to stop the reaction and the solution was filtered with a vacuum flask. Both final solutions GelMA and AlgMa were lyophilized and stored at −20°C, Both were mixed at different concentrations and then diluted in sterile PBS (Gibco) containing the photoinitiator lithium phenyl (2,4,6-trimethylbenzoyl) phosphinate (LAP) (TCI Europe N. V.) at 0.025% (w/v), as described elsewhere (García-Lizarribar et al., 2018; Lafuente-Merchan et al., 2021). These polymer solutions were placed at 65°C for 1 h to obtain homogeneous solutions at 2% and 5% (w/v) GelMA and 1% (w/v) AlgMA, and further combined with other hydrogels as described in Table 1. Volume ratios were set at: 0.5 mL of either GelMA or AlgMA (with LAP), 0.5 mL HA (with or without glycerol), 0.8 mL fibrin (by combining 0.5 mL fibrinogen and 0.3 mL diluted thrombin), and 0.5 mL of MSC, bone marrow (BM) suspension in saline solution.

2.2 | Cells and cell culture

In this study, we used two lines of clinical grade human BM-derived MSCs (MSC, BM) from a master cell bank (passage 5) that were generated following established methods for isolation, expansion, and characterization in the context of a clinical trial for testing a TEP composed of bone particles, fibrin, and MSC, BM in osteonecrosis of the femoral head (ClinicalTrial.gov Id. NCT01605383, EudraCT No. 2010-023998-18) with appropriate donor informed consent for further use in biomedical research (Codinach et al., 2016; García-Muñoz & Vives, 2021). The required number of cells was achieved using expansion medium consisting of Dulbecco's Modified Eagle's Medium (Gibco) containing 2 mM glutamine and supplemented with 10% (v/v) pooled human serum B (hSerB; Banc de Sang i Teixits). All cultures were maintained at 37°C, 5% CO_2 and 95% humidity. Medium was changed every 2–4 days. Cell number and viability were determined by the haemocytometer-based Trypan Blue dye exclusion assay or using Perfect-Count Microspheres (Cytognos SL) in a FACSCalibur cytometer (Becton Dickinson). Viability was determined by cytometry using the 7-Amino-Actinomycin D (7-AAD; BD Biosciences) exclusion method and expressed as a percentage (%) of total cells. Data were analyzed with the CellQuest Pro software (Becton Dickinson).

2.3 | Phenotype assessment

Immunophenotypic characterization of MSC, BM was performed using the following antibodies: mouse anti-human CD45-fluorescein isothiocyanate (CD45-FITC; HI30; BD Pharmingen), anti-human CD105-phycoerythrin (CD105-PE; 43A4E1; Miltenyi Biotec), anti-human HLA-DR$^-$FITC (L243; BD Biosciences), anti-human CD90-PE (F15$^-$42-1$^-$5; Beckman Coulter), anti-human CD31-FITC (WM59; BD Pharmingen), and anti-human CD73-PE (AD2; BD Pharmingen). Double stainings were performed to better define regions of positivity for each marker, as follows: CD90$^+$/HLA-DR,$^-$ CD105$^+$/CD45,$^-$ and CD73$^+$/CD31.$^-$ Cells were stained for 15 min at room temperature, washed and resuspended in PBS. Nonspecific cell staining was ruled out by using mouse immunoglobulin isotype controls (BD Pharmingen). Acquisition was done using a FACSCalibur and data were analyzed with the CellQuest Pro software (Becton Dickenson).

TABLE 1 Matrix of conditions tested to identify a bioprintable zone for mesenchymal stromal cells.

Group	GelMA % (w/v)	AlgMA % (w/v)	LAP % (w/v)	HA % (w/v)	Glycerol (UI/mL)	Thrombin (UI/mL)	Fibrin (mg/mL)
1	5	1	0.025	0	0.5	0.25	5
2	5	1	0.025	0	0.5	0.25	5
3	5	1	0.025	0.8	0.5	0.25	5
4	2	0	0.025	0.8	0.5	0.25	5
5	0	0	0	0.8	0.5	0.25	5

Note: Fibrin resulted from activation of fibrinogen with diluted thrombin solution.

Abbreviations: AlgMA, alginate methacryloyl; GelMA, gelatin methacryloyl; HA, hyaluronic acid; LAP, lithium phenyl (2,4,6-trimethylbenzoyl) phosphinate.

2.4 | Differentiation assays and staining

StemPro differentiation media (Gibco) were used for the osteogenic, chondrogenic, and adipogenic induction of undifferentiated MSC, BM cultures in vitro. Alkaline phosphatase (ALP; Takara Bio Inc.), Alizarin red (EMD Millipore), Safranin O (Sigma-Aldrich), and Oil Red O (Sigma-Aldrich) stainings were performed for the determination of the outcome of the differentiation assays. Differentiation experiments were performed in triplicates.

2.5 | Generation of 3D constructs

1×10^6 MSCs were resuspended in 0.5 mL of Plasmalyte 148 saline solution supplemented with 2% (w/v) HSA (Albutein; Grifols). The cell suspension was then mixed with the help of a viscous liquid pipette with 0.5 mL of hydrogel combinations described in Table 1 and 0.5 mL of activated fibrinogen (TissuCol Duo; Grifols). Then, 5 x 5 x 1.2 mm grids were printed as a model structure using a bioprinter 3DDiscovery BioSafety (regenHU; 365 nm, 3 W/cm^2) with or without UV light.

2.6 | Cell viability and proliferation assessment

Samples of 0.2 and 0.4 cm^3 were dispensed onto nonadherent 24-well plates (Sarstedt). Wells were filled with 1 mL of expansion medium and cultured for up to 7 days at 37°C, 5% CO_2 and 95% humidity. Cell viability was assayed both by (i) determining ATP content with the CellTiter-Glo® 3D Cell Viability Assay (Promega) and (ii) microscopic inspection upon staining with the Live/Dead Viability/Cytotoxicity Kit for mammalian cells (Life Technologies), at three different time points, namely 0, 3, and 7 days after 3D bioprinting, as briefly described next. For the ATP assay, 0.4 cc size constructs were assayed in a final volume of 1 mL (0.5 mL of expansion media and 0.5 mL of ATP reagent), according to the manufacturer's recommendations. Upon stabilization of the ATP reaction, 100 µL samples were assayed in triplicates in a Tecan Spark luminometer equipped with SparkControl software (Tecan GmbH). Please note that relative light units (RLU) do not have any physical meaning and, regardless of the absolute RLU value, we measured the increase of (RLU) over time as an indicator of cellular proliferation. On the other hand, 0.2 cm^3 size constructs were assayed in triplicates by Live/Dead assay according to the manufacturer's recommendations. First, expansion media was removed and washed out with Life Cell Imaging Solution 1x (LCiS) (Life Technologies) and stained for 30 min at 37°C using LCiS containing Ethidium Bromide-homodimer and calcein. After staining, constructs were incubated with PBS containing fluorescent nuclear staining Hoechst 33342 (Life Technologies) for 10 min at room temperature, followed by two washes with PBS. After mounting with 10% glycerol solution (Sigma-Aldrich), at least 4 images per replicate were captured in a Leica DM IL LED (Leica Microsystems) fluorescent microscope.

2.7 | Analysis of the mechanical properties of composite hydrogels

Uniaxial compression tests of hydrogels were performed using a Zwick Z0.5 TN instrument (Zwick-Roell) with a 5N load cell as described elsewhere (García-Lizarribar et al., 2018). Briefly cylindrical hydrogels were cut using a biopsy punch and samples were tested at room temperature up to 30% final strain (deformation), using the following parameters: 0.1 mN preload force and 20% min^{-1} strain rate. Values for the compressive modulus were calculated from the slope of the linear region corresponding to 10%–20% strain. For each hydrogel formulation, three samples were prepared, and measurements were performed in triplicate.

3 | RESULTS AND DISCUSSION

3.1 | Cell production

Human MSC, BM cells were successfully thawed and expanded up to sufficient numbers from a GMP-grade master cell bank with 96.3% viability, displaying surface marker profile compatible with mesenchymal identity (99.9% CD105$^+$/CD45,$^-$ 10.3% HLA-DR,$^+$ 100.0% CD90,$^+$ and 99.2% CD73$^+$/CD31$^-$). Regarding multipotency, MSC, BM readily differentiated into cartilage, fat, and bone-like tissues as determined in vitro using specific lineage induction media and Safranin O (stains proteoglycans, chondrocytes, and type II collagen in varying shades of red), Oil Red O (stains neutral triglycerides and lipids), and Alizarin red (stains calcium deposits) tissue specific stainings (Supporting Information: Figure 1). Altogether, compliance with this quality control panel for identity and potency of MSC, BM confirmed their suitability for use in the study.

3.2 | Effect of 3D bioprinting on cell viability

A matrix of experiments combining different hydrogels and 1×10^6 viable MSC, BM (resuspended in 0.5 mL) was conducted to evaluate the effect of 3D bioprinting of a model grid shape on cell viability. All runs of the experimental design were successfully executed yielding constructs with distinctively different outlooks and variable cell recovery and viability, as depicted in Figure 1a. In gorups 1 and 2, the constructs were easy to handle and retained their macroscopic grid appearance. However, cell viability was dramatically affected resulting in few observable cells, being dead most of them, as revealed by Live/Dead staining resulting in viabilities of 19.53% and 47.13%, respectively. Conversely, groups 3–5 displayed higher viabilities (57.97%, 96.48%, and 96.94%, respectively) (Figure 1b). Remarkably, the number of viable cells was above 50% in these three experimental groups. These observations are compatible with our understanding of the behavior of highly viscous and printable materials. In groups 1 and 2, the high concentration of polymers is likely to yield matrices with close porous environment that impede the migration and proliferation of the encapsulated cells or even nutrient

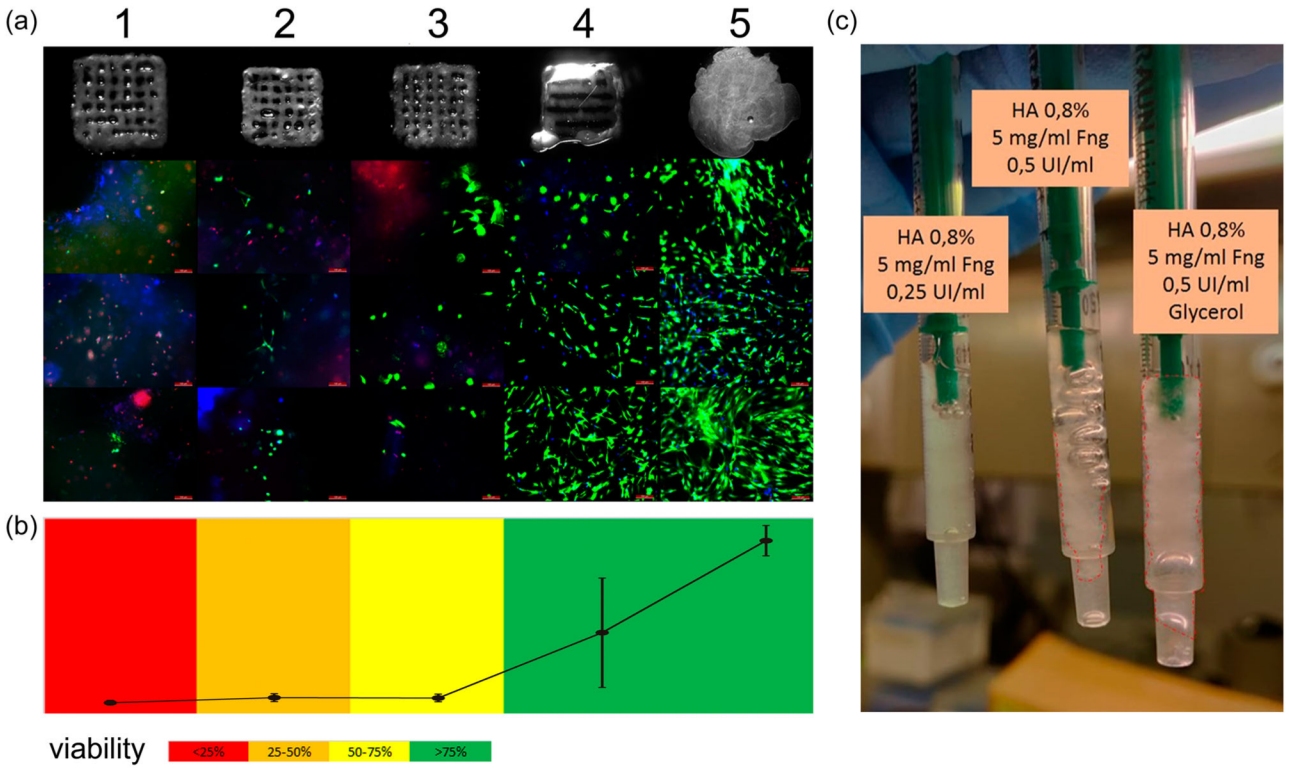

FIGURE 1 Effects of bioink composition on product shape, cell recovery, and cell viability. (a) The combinations of hydrogels that supported highly defined 3D structures (groups 1 and 2) were associated to low cell recovery with poor viability, whereas groups 3 and 4 displayed a compromise of shape resolution, viable cell recovery, and viability (percentages are shown in color code). This is graphically shown by representing viable cell number and overall viability for each condition in (b). Interestingly, the addition of glycerol and/or hyaluronic acid (HA) in the formulation of bioinks contribute to visually more homogeneous mixtures (c). Fng, fibrinogen; 3D, three dimensional.

diffusion. Indeed, formulations from groups 1 and 2 displayed compression modules of 13.8 ± 0.3 and 8.8 ± 0.5 kPa ($n = 3$), respectively. Interestingly, the addition of glycerol and HA in the mixture of hydrogels resulted in highly homogeneous blends as determined visually from their macroscopic appearance (Figure 1c). Consequently, two formulations showing a balanced compromise between defined 3D bioprinted structure and viable cell recovery were chosen for the next phase of the study of bioinks in which proliferation and osteogenic potential was further assessed in vitro.

3.3 | Assessment of proliferation and osteogenic potential

Next two optimal formulations were chosen: 1×10^6 BM, MSC resuspended in 0.5 mL of Plasmalyte 148 supplemented with 2% (w/v) HSA; 0.5 mL of either 5% (w/v) GelMA (formulation "Gel") or 5% (w/v) HA (formulation "HA"); 0.5 mL of 5 mg fibrinogen/mL activated with 0.3 mL of 0.25 UI thrombin/mL. This way, 3D constructs were successfully bioprinted by fused deposition modeling using filaments from both bioink formulations. Conditions during the printing process can potentially affect cell viability, such as thermal damage during the printing process and the mechanical forces applied during extrusion. By visual inspection, the definition of the 3D architecture was superior using GelMA (Figure 2a) and, in both cases, bioprinted MSC, BMs appeared as viable spherical cells, homogenously distributed within the 3D construct without any sign of cell death, as determined by Live/Dead staining at Day 0 (Figure 2b). The maintenance of the proliferation capacity of 3D printed MSC, BMs was demonstrated for both bioinks by a steady increase of ATP content at Days 3 and 7 in expansion medium for HA constructs whereas Gel constructs did not allow for sustained proliferation most likely as result of the dense printed structure that impeded migration of cells (Figure 2c). Remarkably, the characteristic fibroblastic morphology of MSCs was acquired already by Day 3 and cells populated the entire 3D structure homogenously (Figure 2b). Importantly, MSCs also retained their osteogenic capacity as evidenced by the presence of ALP^+ positive cells, reaching a peak of ALP activity at Week 2 after osteogenic induction in vitro. Such differentiation profile of an early osteogenic marker is comparable to the behavior of MSC, BM undergoing planar osteogenic differentiation, demonstrating the preservation of potency in 3D bioprinted structures (Figure 2d).

3.4 | Quality and regulatory implications of using natural hydrogels in 3D bioprinting

Cell-based therapies are rapidly evolving from traditional use in blood transfusion or transplantation of hematopoietic progenitors and

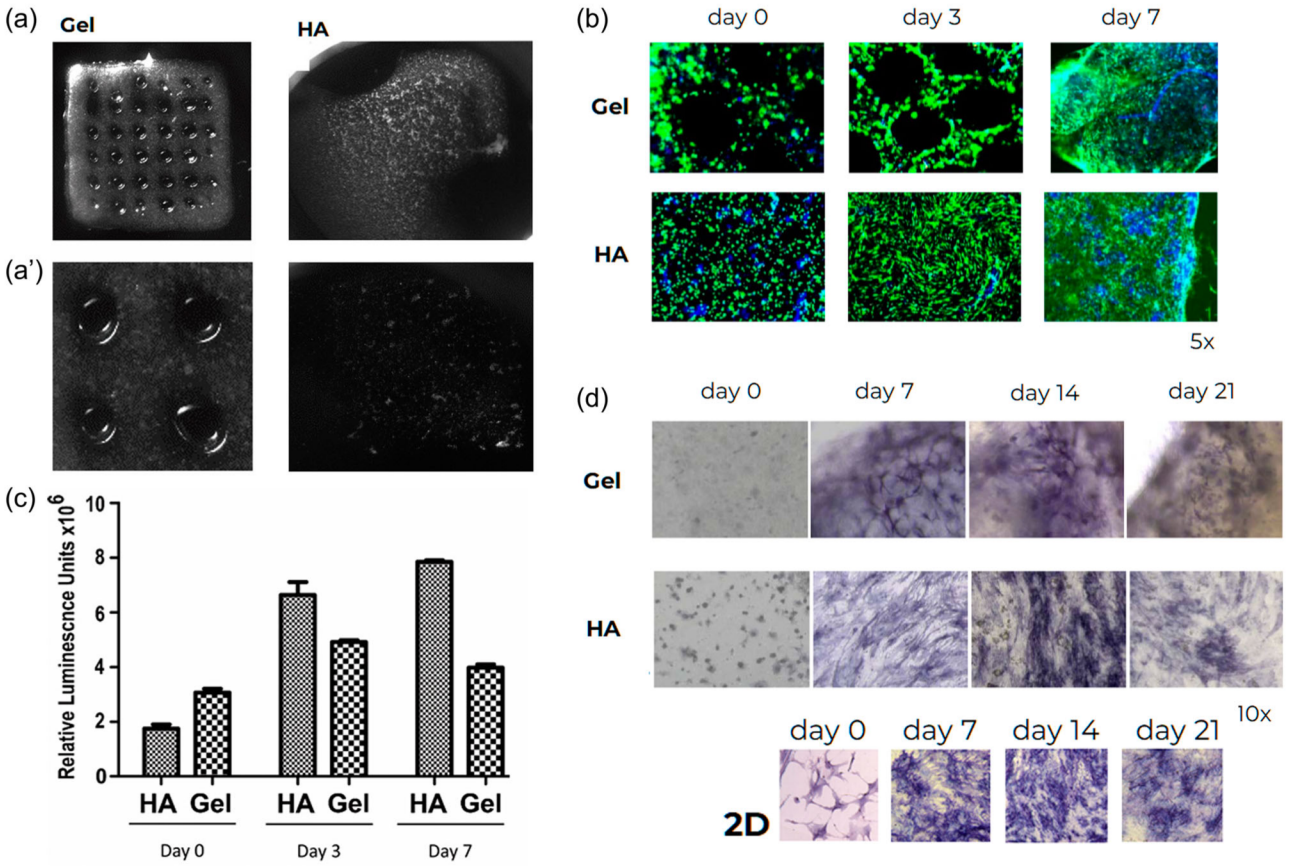

FIGURE 2 Effect of 3D printing on viability and potency of human bone marrow-derived multipotent MSC. In (a), macroscopic appearance of 3D printed grid-shape constructs (zoomed in a'). Cell proliferation was achieved in bioprinted constructs resulting from the use of the two selected hydrogel formulations (Gel and HA) whereas bioink formulated with gelatin (Gel) favored rapid proliferation in the first 3 days after bioprinting but failed to sustain high numbers of cells in culture at Day 7 (b, c). Cell viability was very high in both conditions (representative images from triplicates of Live/Dead staining, at indicated time points; x5 magnification) (b). Osteogenic commitment of human MSC, BMs remained unaltered after 3D bioprinting in both conditions (representative images from triplicates are shown in (d), at different time points, x10), showing a peak of alkaline phosphatase (ALP^+) activity at Day 14 postinduction of osteogenic in vitro differentiation (d), comparable to the differentiation profile observed in planar cultures (2D). BM, bone marrow; MSC, mesenchymal stromal cells; 3D, three dimensional.

tissues to today's innovative ATMP. Therapeutic activity of this new category of medicines is primarily based on the preservation of cell viability, which limits shelf-life and accounts for the complex logistics to ensure that drug products remain within specifications at the time of administration, typically within 24 h from batch release (Mirabel et al., 2018). Identification of CQAs, such as viability, is the first and most difficult step in the implementation of quality by design (QbD) for development and production of ATMPs (Lipsitz et al., 2016). The list of potential CQAs is commonly modified along the life cycle of ATMP development, as better product knowledge and process understanding are gained. In this context, quality risk management can be used to prioritize the list of potential CQAs for subsequent evaluation (Vives & Amposta, 2021). Therefore the cell's CQAs are defined according to their impact on the product's safety profile and clinical efficacy, and how these are perturbed by any disturbance in the process (Williams et al., 2016).

Although 3D bioprinting technologies offer the possibility to automate cell-based TEP manufacture, the election of hydrogels is not trivial and must rely on their ability to: (i) protect cells from mechanical stress; and (ii) offer a microenvironment for cells to recapitulate biological processes, such as proliferation and differentiation into tissue specific cells. It is unlikely that a single hydrogel would meet all the desirable properties for tissue engineering. For instance, GelMA lacks biomechanical versatility and lasting 3D structures. For this reason, we investigated hydrogel blends to obtain versatile, lasting, mechanically tunable scaffolds that maintain the CQAs of 3D bioprinted osteogenic cell-based structures. Particularly, the main reason for using natural hydrogels such as fibrinogen is due to their potential to mimic physiological conditions as a result of their biocompatibility and resorbability, as well as being readily available commercially in clinical grade (e.g., Baxter's Tissel/Tissucol). Indeed human fibrin is useful as a matrix for cell delivery in tissue engineering strategies either alone or in combination with other materials, such as polycaprolactone or hyaluronan (S. H. Park et al., 2011; S. Y. Park et al., 2016). Particularly MSC combined with fibrin can facilitate the implantation in bone defect reconstruction,

cartilage, and tendon injury repair through: (i) its potential to generate new tissue (via differentiation), and/or (ii) the capacity to modulate responses (via paracrine signaling) either locally or systemically (Nombela-Arrieta et al., 2011). The combination with other hydrogels, particularly HA that also meets biocompatibility, biomechanical, and regulatory criteria to be used as bioinks contributed to the preservation of CQAs in osteogenic 3D printed MSC, BM-based products.

Despite much progress in the field, the optimal range of compression modules for optimal 3D bone bioprinting are largely unknown provided that TEP can either (i) be transplanted as such (then mechanical characteristics should either resemble as much as possible those of native bone or capable to mature in vivo) or (ii) matured ex vivo (then mechanical characteristics should be optimal for cell proliferation, differentiation, and synthesis of extracellular matrix).

The novelty of our approach is (i) the demonstration that 3D bioprinted cells preserve their regenerative attributes, and (ii) its practical clinical translatability, due to the use of natural hydrogels that can be readily adapted to clinical grade formulation. To move towards clinical testing, further work confirming safety and efficacy in translational animal models will be required. Despite potential limitations in scalability to satisfy future clinical demand, the extrusion-based methods used in this work has been selected from presently available 3D bioprinting strategies most likely to meet clinical-scale needs. Indeed, another limitation that needs to be acknowledged before clinical use is the in vitro nature of the present study and therefore the requirement for further evaluation in translational animal models, which would provide evidence of feasibility, safety, and efficacy, as we have reported previously for manually modeled 3D constructs (Prat et al., 2018).

4 | CONCLUSIONS

Beyond the biocompatibility of naturally occurring polymers, our results highlight the enhanced protection on MSC, BM viability exerted by bioinks of natural origin (preferably HA, gelatin, and fibrin) during the 3D bioprinting process, by reducing shear stress and offering structural support for proliferation and osteogenic differentiation. Specifically, 3D structures with a compression modulus below 8.8 ± 0.5 kPa define a suitable "bioprintable zone" for optimal preservation of CQA.

AUTHOR CONTRIBUTIONS

Patricia Gálvez-Martín, Josep Samitier, and Joaquim Vives conceived the study. Lluís Martorell, Alba López-Fernández, and Andrea García-Lizarribar performed experiments. Roger Sabata, Patricia Gálvez-Martín, Josep Samitier, and Joaquim Vives analyzed data. Joaquim Vives wrote the original draft. Lluís Martorell, Alba López-Fernández, Josep Samitier, and Joaquim Vives revised and edited the manuscript. All authors have read and agreed to the submitted version of the manuscript.

ACKNOWLEDGMENTS

The authors would like to acknowledge Clara Frago (BST) for their assistance with the assessment of the trilineage differentiation potential of MSC, BM; MicroFabSpace and Microscopy Characterization Facility, Unit 7 of ICTS "NANBIOSIS" from CIBER-BBN at IBEC; and Dr. Màrius Aguirre (VHIR) for facilitating this collaborative work. This work has been developed in the context of AdvanceCat and Base 3D with the support of ACCIÓ (Catalonia Trade & Investment; Generalitat de Catalunya) under the Catalonian ERDF operational program (European Regional Development Fund) 2014–2020. Research in JV's laboratory is developed in the context of Red Española de Terapias Avanzadas (TERAV, expedient no. RD21/0017/0022) funded by Instituto de Salud Carlos III (ISCIII) in the context of NextGenerationEU's Recovery, Transformation and Resilience Plan. This work was supported by Networking Biomedical Research Center (CIBER), Spain. CIBER is an initiative funded by the VI National R&D&i Plan 2008–2011, Iniciativa Ingenio 2010, Consolider Program, CIBER Actions, and the Instituto de Salud Carlos III (RD16/0006/0012), with the support of the European Regional Development Fund; CERCA Program and by the Commission for Universities and Research of the Department of Innovation, Universities, and Enterprise of the Generalitat de Catalunya (2017 SGR 719 and 2017 SGR 1079).

CONFLICT OF INTEREST STATEMENT

The authors decalre no conflict of interest.

DATA AVAILABILITY STATEMENT

The data that support the findings of this study are available from the corresponding author upon reasonable request.

ETHICS STATEMENT

Bone marrow aspirates were donated with appropriate informed consent; both human and ovine mesenchymal stromal cells were generated from bone marrow following protocols approved by Vall d'Hebron Ethical Committee for use in biomedical research.

ORCID

Lluís Martorell http://orcid.org/0000-0001-9348-4531
Alba López-Fernández http://orcid.org/0000-0001-6072-0294
Andrea García-Lizarribar http://orcid.org/0000-0001-5072-2093
Roger Sabata http://orcid.org/0000-0002-4769-4615
Patricia Gálvez-Martín http://orcid.org/0000-0001-9724-8560
Josep Samitier http://orcid.org/0000-0002-1140-3679
Joaquim Vives http://orcid.org/0000-0001-9719-5235

REFERENCES

Abu Owida, H. (2022). Developments and clinical applications of biomimetic tissue regeneration using 3D bioprinting technique. *Applied Bionics and Biomechanics*, *2022*, 2260216. https://doi.org/10.1155/2022/2260216

Cidonio, G., Glinka, M., Dawson, J. I., & Oreffo, R. O. C. (2019). The cell in the ink: Improving biofabrication by printing stem cells for skeletal

regenerative medicine. *Biomaterials*, *209*, 10–24. https://doi.org/10.1016/j.biomaterials.2019.04.009

Codinach, M., Blanco, M., Ortega, I., Lloret, M., Reales, L., Coca, M. I., Torrents, S., Doral, M., Oliver-Vila, I., Requena-Montero, M., Vives, J., & Garcia-López, J. (2016). Design and validation of a consistent and reproducible manufacture process for the production of clinical-grade bone marrow-derived multipotent mesenchymal stromal cells. *Cytotherapy*, *18*(9), 1197–1208.

Dimarino, A. M., Caplan, A. I., & Bonfield, T. L. (2013). Mesenchymal stem cells in tissue repair. *Frontiers in Immunology*, *4*, 201. https://doi.org/10.3389/fimmu.2013.00201

Donnaloja, F., Jacchetti, E., Soncini, M., & Raimondi, M. T. (2020). Natural and synthetic polymers for bone scaffolds optimization. *Polymers*, *12*(4), 905. https://doi.org/10.3390/polym12040905

García de Frutos, A., González-Tartière, P., Coll Bonet, R., Ubierna Garcés, M. T., Del Arco Churruca, A., Rivas García, A., Matamalas Adrover, A., Saló Bru, G., Velazquez, J. J., Vila-Canet, G., García-Lopez, J., Vives, J., Codinach, M., Rodriguez, L., Bagó Granell, J., & Càceres Palou, E. (2020). Randomized clinical trial: Expanded autologous bone marrow mesenchymal cells combined with allogeneic bone tissue, compared with autologous iliac crest graft in lumbar fusion surgery. *The Spine Journal*, *20*(12), 1899–1910. https://doi.org/10.1016/j.spinee.2020.07.014

García-Lizarribar, A., Fernández-Garibay, X., Velasco-Mallorquí, F., Castaño, A. G., Samitier, J., & Ramon-Azcon, J. (2018). Composite biomaterials as long-lasting scaffolds for 3D bioprinting of highly aligned muscle tissue. *Macromolecular Bioscience*, *18*(10), 1800167. https://doi.org/10.1002/mabi.201800167

García-Muñoz, E., & Vives, J. (2021). Towards the standardization of methods of tissue processing for the isolation of mesenchymal stromal cells for clinical use. *Cytotechnology*, *73*(3), 513–522. https://doi.org/10.1007/s10616-021-00474-3

Jose, R. R., Rodriguez, M. J., Dixon, T. A., Omenetto, F., & Kaplan, D. L. (2016). Evolution of bioinks and additive manufacturing technologies for 3D bioprinting. *ACS Biomaterials Science & Engineering*, *2*(10), 1662–1678. https://doi.org/10.1021/acsbiomaterials.6b00088

Lafuente-Merchan, M., Ruiz-Alonso, S., Espona-Noguera, A., Galvez-Martin, P., López-Ruiz, E., Marchal, J. A., López-Donaire, M. L., Zabala, A., Ciriza, J., Saenz-del-Burgo, L., & Pedraz, J. L. (2021). Development, characterization and sterilisation of Nanocellulose-alginate-(hyaluronic acid)-bioinks and 3D bioprinted scaffolds for tissue engineering. *Materials Science and Engineering: C*, *126*, 112160. https://doi.org/10.1016/j.msec.2021.112160

Lipsitz, Y. Y., Timmins, N. E., & Zandstra, P. W. (2016). Quality cell therapy manufacturing by design. *Nature Biotechnology*, *34*(4), 393–400. https://doi.org/10.1038/nbt.3525

Mirabel, C., Puente-Massaguer, E., Del Mazo-Barbara, A., Reyes, B., Morton, P., Gòdia, F., & Vives, J. (2018). Stability enhancement of clinical grade multipotent mesenchymal stromal cell-based products. *Journal of Translational Medicine*, *16*(1), 291. https://doi.org/10.1186/s12967-018-1659-4

Murphy, S. V., & Atala, A. (2014). 3D bioprinting of tissues and organs. *Nature Biotechnology*, *32*(8), 773–785. https://doi.org/10.1038/nbt.2958

Nombela-Arrieta, C., Ritz, J., & Silberstein, L. E. (2011). The elusive nature and function of mesenchymal stem cells. *Nature Reviews Molecular Cell Biology*, *12*(2), 126–131.

Park, S. H., Choi, B. H., Park, S. R., & Min, B. H. (2011). Chondrogenesis of rabbit mesenchymal stem cells in fibrin/hyaluronan composite scaffold in vitro. *Tissue Engineering. Part A*, *17*(9–10), 1277–1286. https://doi.org/10.1089/ten.TEA.2010.0337

Park, S. Y., Choi, J. W., Park, J. K., Song, E. H., Park, S. A., Kim, Y. S., Shin, Y. S., & Kim, C. H. (2016). Tissue-engineered artificial oesophagus patch using three-dimensionally printed polycaprolactone with mesenchymal stem cells: A preliminary report. *Interactive Cardiovascular and Thoracic Surgery*, *22*(6), 712–717.

Prat, S., Gallardo-Villares, S., Vives, M., Carreño, A., Caminal, M., Oliver-Vila, I., Chaverri, D., Blanco, M., Codinach, M., Huguet, P., Ramírez, J., Pinto, J. A., Aguirre, M., Coll, R., Garcia-López, J., Granell-Escobar, F., & Vives, J. (2018). Clinical translation of a mesenchymal stromal cell-based therapy developed in a large animal model and two case studies of the treatment of atrophic pseudoarthrosis. *Journal of Tissue Engineering and Regenerative Medicine*, *12*(1), e532–e540. https://doi.org/10.1002/term.2323

Vivas, D., Grau-Vorster, M., Oliver-Vila, I., García-López, J., & Vives, J. (2020). Evaluation of a cell-based osteogenic formulation compliant with good manufacturing practice for use in tissue engineering. *Molecular Biology Reports*, *47*(7), 5145–5154. https://doi.org/10.1007/s11033-020-05588-z

Vives, J., & Amposta, J. (2021). Risk management. In M. Aljurf, J. A. Snowden, P. Hayden, K. H. Orchard, & E. McGrat (Eds.), *Quality management and accreditation in hematopoietic stem cell transplantation and cellular therapy: The JACIE guide* (pp. 165–176). Springer. https://doi.org/10.1007/978-3-030-64492-5_18

Vives, J., & Mirabel, C. (2019). Multipotent mesenchymal stromal cells from bone marrow for current and potential clinical applications. In R. L. Reis (Ed.), *Encyclopedia of tissue engineering and regenerative medicine* (pp. 503–512). Academic Press. https://doi.org/10.1016/B978-0-12-801238-3.65506-X

Vives, J., Rodriguez, L., Coca, M. I., Reales, L., Cabrera-Perez, R., & Martorell, L. (2021). Use of multipotent mesenchymal stromal cells, fibrin, and scaffolds in the production of clinical grade bone tissue engineering products. *Methods in Molecular Biology*, *2286*, 251–261. https://doi.org/10.1007/7651_2020_280

Williams, D. J., Archer, R., Archibald, P., Bantounas, I., Baptista, R., Barker, R., Barry, J., Bietrix, F., Blair, N., Braybrook, J., Campbell, J., Canham, M., Chandra, A., Foldes, G., Gilmanshin, R., Girard, M., Gorjup, E., Hewitt, Z., Hourd, P., … Zimmerman, H. (2016). Comparability: Manufacturing, characterization and controls, report of a UK regenerative medicine platform pluripotent stem cell platform workshop, trinity hall, cambridge, 14–15 September 2015. *Regenerative Medicine*, *11*(5), 483–492. https://doi.org/10.2217/rme-2016-0053

SUPPORTING INFORMATION

Additional supporting information can be found online in the Supporting Information section at the end of this article.

How to cite this article: Martorell, L., López-Fernández, A., García-Lizarribar, A., Sabata, R., Gálvez-Martín, P., Samitier, J., & Vives, J. (2023). Preservation of critical quality attributes of mesenchymal stromal cells in 3D bioprinted structures by using natural hydrogel scaffolds. *Biotechnology and Bioengineering*, *120*, 2717–2724. https://doi.org/10.1002/bit.28381